



Control Technology and Simulation Study of Floor Heave in High Stress Soft Rock Roadway

Laizheng Xu · Sijiang Wei

Received: 14 February 2020 / Accepted: 11 March 2020 / Published online: 23 March 2020
© Springer Nature Switzerland AG 2020

Abstract In order to solve the problems of large deformation and difficult control of the soft rock roadway floor under the influence of high stress and mining stress superposition in Zhaogu mining area, this paper analyzes the stress environment and failure mechanism of the surrounding rock by means of on-site investigation, numerical simulation and on-site industrial test. It is considered that the floor heave of the soft rock roadway is the result of the joint action of the surrounding rock fracture development, poor lithology, cementation, low strength of the original support and high ground stress. The distribution characteristics of stress, displacement and plastic zone of surrounding rock in soft rock roadway under different stress and support mode are analyzed by numerical simulation. Based on the above analysis, the combined control technology of “prestressed grouting anchor cable + grouting anchor bolt + grouting behind the wall + floor reconstruction” is proposed to effectively control the occurrence of roadway floor. The data of monitoring verifies that the grouting bolt

changes the structure of broken coal and rock mass on the floor and restrains the occurrence of floor heave.

Keywords High stress · Soft rock · Floor heave · Numerical simulation · On-site monitoring

1 Introduction

With the depletion of the shallow coal resources, the exploitation of the coal resources gradually develops to the deep, and the corresponding engineering geological conditions are increasingly complex (Zhang 2005), resulting in the maintenance difficulty of the surrounding rock support of the large section roadways and chambers, and the heavy workload of the repair, which not only brings great safety risks, but also seriously hinders the production efficiency. Under the deep environment, the ground stress of the roadway increases correspondingly, and the original rock stress has a great influence on the stability of the surrounding rock of the roadway (Ma and Hou 1995). The surrounding rock of the deep coal roadway forms engineering soft rock under the strong original rock stress (He and Sun 2004), and the serious floor heave is one of the development problems.

Scholars at home and abroad have done a lot of research on the control of deep roadway and chamber surrounding rock. In terms of new support means, the paper puts forward concrete-filled steel tube support

L. Xu · S. Wei (✉)
School of Energy Science and Engineering, Henan
Polytechnic University, Jiaozuo 454003,
Henan, China
e-mail: jzitwsj@126.com

L. Xu
Jiaozuo Coal Industry Group Co., Ltd, Jiaozuo 454000,
Henan, China

(Liu et al. 2017a, b), strong bolt support (Wu et al. 2017), extendable bolt (Wang et al. 2016), constant resistance large deformation bolt (cable) (He et al. 2014), etc., which has been applied in the complex conditions of soft rock large deformation roadway and chamber (Hao et al. 2016; Zhang et al. 2016a), dynamic pressure affected roadway (Zhang et al. 2016b), chamber group reinforcement (Kang et al. 2011). In terms of the concept of surrounding rock reinforcement in weak roadway, scholars at home and abroad put forward support ideas such as coupling support (He et al. 2013), key part support (Sun and He 2005), composite support (Wei et al. 2013; Liu et al. 2017a, b), and collaborative support (Long et al. 2012). Zhang (2016) put forward the support principle of “two high and one large” in view of the large deformation of the fault broken coal rock roadway. Zheng et al. (2018) designed a composite structure, including concrete antiarches and bolts to control the floor heave. Guo et al. (2017) put forward the comprehensive treatment methods of the grouting bolt combined with reinforcing sidewalls and corners for the floor heave. Yan et al. (2016) proposed that “advance grouting, shotcreting and anchoring grouting stage reinforcement is the foundation support, and then the key parts of anchor cable reinforcement and surrounding rock grouting technology are implemented”. Meng et al. (2017) put forward the technical scheme of “primary steel mesh spraying + reinforced concrete lining + secondary grouting” combined support for the difficult problem of roadway passing through faults under complex geological conditions. Song et al. (2018) used the theory of ultra-low friction effect of rock mass and the theory of dynamic load stress wave to study the influence of dynamic load on fault fracture zone, and put forward the corresponding safety measures of roadway passing through fault. Wang et al. (2019) put forward a comprehensive repair and support scheme, which optimizes the full section support with the technology of bolt mesh cable spraying + concrete filled steel tube support and strengthens the floor support with the reinforced concrete bottom beam. The above research results can provide important reference for the surrounding rock control of roadway and chamber under the deep complex conditions, but due to the complexity of the engineering geological conditions, the engineering analogy method often has certain limitations, which must be analyzed for the specific roadway and

chamber, and there are relatively few researches on the combination of support and improvement of the rock structure of the bottom plate of the roadway.

Based on this, this paper studies the deformation mechanism of the soft rock roadway floor by the methods of engineering geological condition analysis, numerical simulation and field test, puts forward the joint reinforcement plan of “prestressed grouting anchor cable + grouting anchor bolt + grouting behind the wall + floor reconstruction”, develops a new type of floor drilling rig, and carries out field monitoring of mine pressure.

2 Deformation Characteristics of Soft Rock Roadway Floor

2.1 Project Overview

The No.11021 working face is located in the western part of the Zhaogu No. 2 Mine. The east side of the lower trough of the No.11021 working face is the inner section of the unearthed No. 11021 working face, the west side is the upper trough of the No.11041 working face, the north is the contact lane of the No.11021 working face, and the south is the F18 fault. The layout of No. 11021 working face is shown in Fig. 1.

The average thickness is 5.8 m of No. 21# coal seam, and the pseudo roof mainly consists of mudstone and carbonaceous mudstone with a thickness less than 0.5 m. The thickness of direct roof is generally 1–6.5 m, mainly mudstone roof. The main roof is coarse, medium and fine sandstone with an average thickness of 7.46 m. The floor is mainly composed of mudstone and sandy mudstone, with an average of 12.84 m. The floor is easy to soften and swell with water. The cracks in the floor are developed with obvious horizontal bedding, the cracks in the floor are developed, and there is old empty water in the tunnel. The conditions of coal seam roof and floor are shown in Table 1.

2.2 Deformation Characteristics of Soft Rock Roadway

After the excavation of the rock mass, the initial deformation rate of the lower channel in the inner section of the No.11021 working face is very large. In a short period of time (generally 3–7 days), the

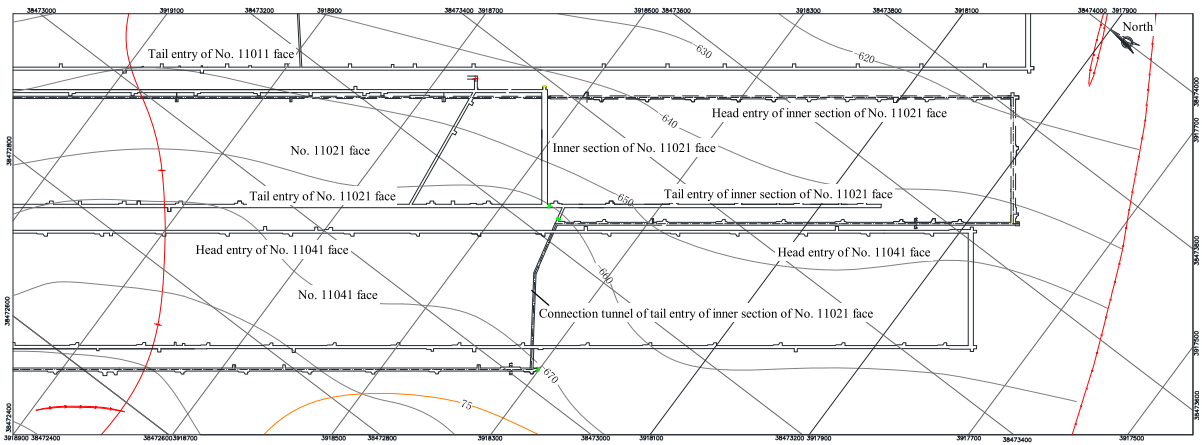


Fig. 1 Schematic diagram of mining engineering in No. 11021 working face

Table 1 Coal seam roof and floor

Position	Name	Average thickness/m
<i>Roof</i>		
Main roof	Fine to coarse sandstone	7.46–14.67
Immediate roof	Sandy mudstone	3.2–6.5
False roof	Mudstone	0–0.5
<i>Floor</i>		
Immediate floor	Sandy mudstone, mudstone	13.73–14.04

deformation can reach 500 mm, and the deformation in some areas can reach 1000 mm, resulting in the condition that the roadway is excavated before and repaired after excavation, the concrete is cracked, the support is damaged seriously, and the roadway has to be expanded and reinforced again, and the damage form of the roadway is shown in Fig. 2. According to the analysis of engineering geological conditions, the reasons for the instability of the inner section of No.11021 working face are as follows:

1. The geological structure and stress environment are complex. The fault is developed near the mining roadway, the buried depth of the roadway is about 700 m, the horizontal stress is 1.2–1.5 times of the vertical stress, the roadway around the mining roadway is crisscross, and the supporting stress between the roadways overlaps with each other, resulting in a large supporting pressure of the rock pillar.



Fig. 2 Bottom drum of lower groove in inner section of 11021 working face

2. The fracture of surrounding rock is developed. In the structural area, the surrounding rock is tensioned and pulled by faults, with developed fissures, broken surrounding rock and poor self-stability.
3. The lithology of surrounding rock is poor and cemented. The lower channel of the inner section of No.11021 working face is mainly composed of mudstone and sandy mudstone. It is greatly affected by water. After encountering water, it will expand and muddy. It has strong softening, sharp reduction of strength and loss of bearing capacity.
4. Rheology of surrounding rock of roadway. The initial support form of roadway surrounding rock is bolting and shotcreting, but due to the untimely shotcreting, the surrounding rock is weathered and even loose, which is easy to cause bolt failure and instability of support structure. Under the action of high stress and fault structural stress, the surrounding rock of roadway changes.
5. The strength of the original support system is low. Although the inner section of No. 11021 working face adopts strong anchoring technology, the surrounding rock has poor anchoring ability, resulting in uneven stress on the support and easy to be broken by each.

3 Soft Rock Roadway Control Mechanism and Support Design

Based on the above analysis, and considering the requirements of simple construction technology and operability, the bottom drum treatment and support scheme is determined as “prestressed grouting anchor cable + grouting anchor bolt + grouting behind the wall + base plate reconstruction”.

3.1 Overall Foundation Reinforcement

The overall reinforcement of roadway foundation adopts full section anchor mesh cable support, as shown in Fig. 3.

1. Roof bolt specification: $\Phi 20 \times 2400$ mm, row spacing of 800×900 mm, bolt tray of $\delta 10 \times 150 \times 150$ mm, used together with steel

ladder, the length of steel ladder is 4160 mm, row spacing of 900 mm.

2. Specification of side anchor cable: $\Phi 17.8 \times 4250$ mm, row spacing of 900×900 mm, tray of 2860 mm long steel ladder and $\delta 12 \times 200 \times 200$ mm steel plate.
3. Specification of anchorage cable of channel steel beam: $\Phi 21.6 \times 8250$ mm, spacing between rows of 1300×1800 mm and 1500×1800 mm, tray of 4200 mm and 3300 mm long 16# channel steel beam and $\delta 12 \times 120 \times 120$ mm, $\delta 12 \times 80 \times 80$ mm steel plate.
4. The top anchor bolt, steel ladder and metal mesh support are closely following the working face; the lag head-on distance of two anchor cables on the upper part of the side shall not exceed two rows; the lag head-on distance of two anchor cables on the lower part of the side shall not be less than five rows, and shall not exceed eight rows.
5. The metal mesh shall be welded with $\Phi 6$ mm steel bars, with mesh size of 1000×1900 mm and overlapping length of not less than 100 mm. It shall be bound firmly with 14# galvanized wire, with top four corners and side corners.

3.2 High Preload Reinforcement Requirements

The anchoring force of all anchor bolts in the tunnel construction is 70 kN, and the bolt torque is not less than 300 N m, the prestressed force of $\Phi 21.6$ mm anchor cable is not less than 350 kN, the prestressed force of $\Phi 17.8$ mm anchor cable is not less than 150 kN.

3.3 Bottom Plate Self Drilling Grouting Anchor Bolt Scheme

Self-drilling grouting anchor has the characteristics of lengthening, self-anchoring, self-drilling, active support, grouting and flexible support. It can be used for advanced support of roadways, radial support, slope reinforcement, roadbed reinforcement, river bank reinforcement, arch angle reinforcement, and roadway disaster rectification projects, as shown in Fig. 4.

The self-drilling anchor consists of four parts: drill bit (anchor head), rod body, fastening device and accessory device, the role of drill bit is drilling and anchoring. The rod body is composed of three parts:

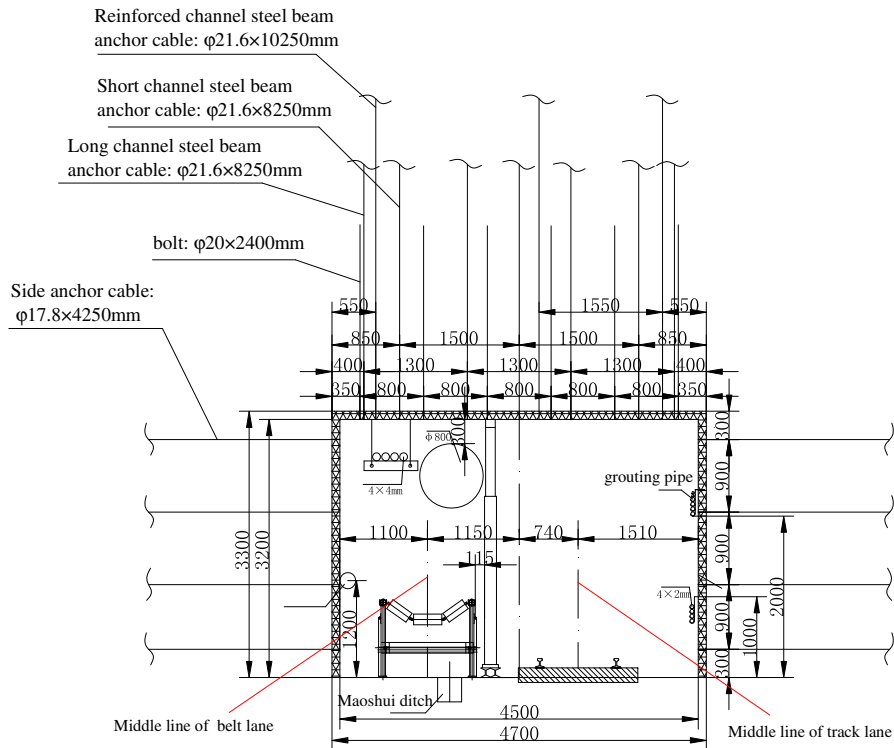
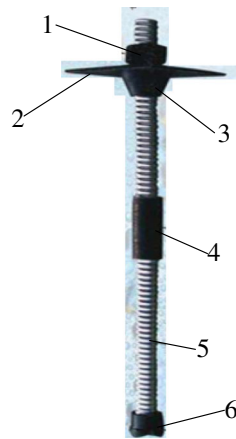


Fig. 3 Cross section of roadway support

Fig. 4 Self drilling anchor



The length of the grouting anchor is set to 4000 mm. At the same time, four small outlets are added to the depth range of 2–4 m of the anchor, and three per row are arranged with a row spacing of 2000 mm, as shown in Fig. 5. The details are as follows: 1# grouting anchor is arranged at 1800 mm to the left of the centerline, and is vertically angled 10°, and the hole depth is 4200 mm. 2# grouting anchor is arranged at 100 mm to the left of the centerline, and the vertical bottom plate is set, and the hole depth is 4200 mm. 3# grouting anchor is placed 500 mm to the right of the center line, tied vertically 30°, and the hole depth is 4200 mm.

drill pipe when drilling, anchor bolt when anchoring, and passage when grouting. At the same time, pre tightening force can be exerted by fastening device. Therefore, the research and development and improvement of the floor bolt equipment provide technical support for the smooth implementation of the deep grouting construction method of the floor. The parameters of grouting anchor bolt in the bottom plate are as follows:

3.4 Prestressed Grouting Anchor Cable Support at the Side

Two rows of reinforced channel beam anchor cables are arranged at the lower side of the roadway. The specification of common anchor cable is $\Phi 17.8 \text{ mm} \times 4250 \text{ mm}$, and the specification of grouting anchor cable is $\Phi 22 \times 4250 \text{ mm}$. The common anchor cable and grouting anchor cable are arranged alternately.

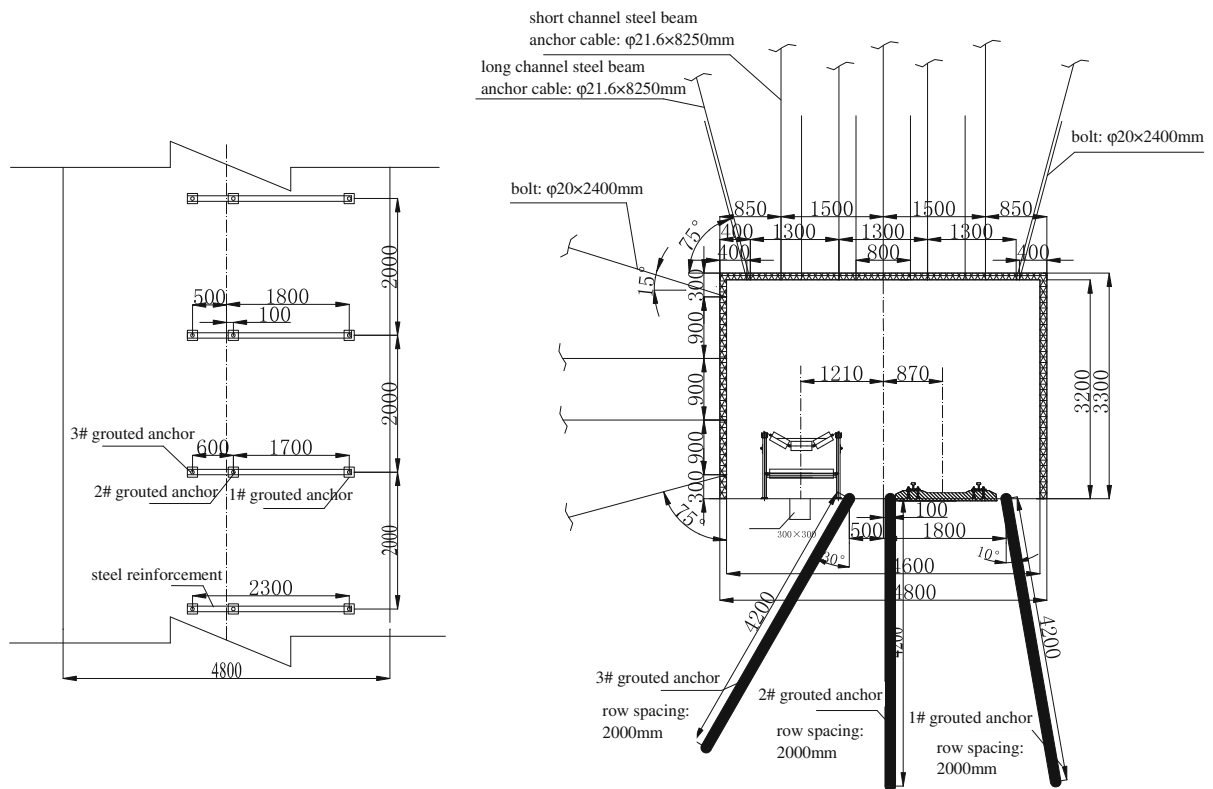


Fig. 5 Cross section of self drilling grouting bolt support of bottom plate

The spacing between the anchor cables is 900 mm, the length of common anchor cable is 1500 mm, and the length of grouting anchor cable is 1000 mm.

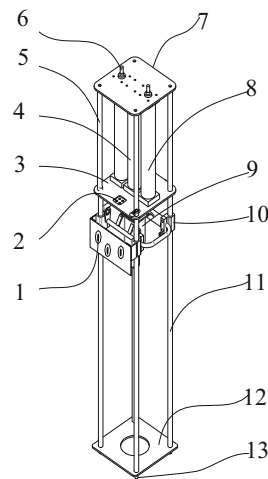
Two rows of reinforced anchor cables are arranged on the upper side of the roadway. The specification of ordinary anchor cable is $\Phi 17.8 \text{ mm} \times 4250 \text{ mm}$, and the specification of grouting anchor cable is $\Phi 22 \times 4250 \text{ mm}$. The ordinary anchor cable and grouting anchor cable are arranged alternately. The spacing between the anchor cables is 900 mm, and the anchorage length of the anchor cable is the same as that of the lower side.

3.5 Development of Drilling Construction Equipment for Bottom Plate

At present, the size of the construction machines and tools for floor drilling is large in size and the construction conditions are high. For example, hydraulic pipes, electric hydraulic pumps, and power distribution equipment need to be laid at the construction site, and there must be a sufficient section of the

roadway. It is forbidden to use live equipment in the return airway. Existing equipment cannot meet the requirements of small aisle space, return airway construction, and the simultaneous deployment of multiple machines in the aisle. Therefore, this paper has developed a floor drilling construction equipment that can solve the above problems. The drilling machine uses the three-dimensional frame to fix the two-way propulsion cylinder and the hand-held pneumatic drilling machine on the same axis, and uses the two-way propulsion cylinder to push up and down, without any external force. It can reduce labor intensity and increase drilling accuracy and depth, as shown in Fig. 6.

Specific usage: Through the external high-pressure air flow, the air flow is divided into three ways to provide power for the air drill, the upper supporting air cylinder and the pushing and pulling air cylinder. First, open the upper supporting hand rotary valve to fix the overall support. Close the supporting cut-off valve, open the hand rotary valve of air drill, adjust the forward and reverse direction of the drilling machine

Fig. 6 Schematic diagram of floor drilling machine

1-hand rotary valve; 2-air hole; 3-intermediate support plate; 4-push-pull cylinder; 5-cylinder support column; 6-upper support cone; 7-upper support plate; 8-upper support cylinder; 9-air drill; 10 slide block; 11-air drill support column; 12-lower support plate; 13-lower support cone

as required, and start the drilling machine for work. Turn the push pull-out hand rotary valve to control the cylinder to slide up and down. Finally, close the air drill, respectively push the pull-out cylinder, and pull the cylinder back.

The main innovations and advantages are: fixed by powerful cylinder, enhanced thrust and better stability. Smaller unit volume, smaller construction area compared with large-scale drilling machine, it can adapt to smaller space area, and can construct multiple units at the same time, greatly improving drilling construction efficiency. The whole structure of the drilling frame is simple and the quality is light, so it can be handled manually.

4 Numerical Simulation Study

4.1 Simulation Analysis Under Different Stress Conditions

4.1.1 Model Establishment

Based on the engineering background of No. 11021 working face of Zhaogu No. 2 mine, a 3D model with the dimension of $X \times Y \times Z = 50 \text{ m} \times 5 \text{ m} \times 37 \text{ m}$ is established by using FLAC^{3D} numerical simulation software. The model is divided into 37,000 units and 45,450 nodes, as shown in Fig. 7. Displacement constraints are applied to the left, right, front, back and bottom boundaries of the model, and uniform load is applied to the top of the model, which is the weight of

the overlying strata. According to the field geological survey and rock mechanics test results, considering the scale effect of rock, the rock mechanics parameters used in the simulation calculation are shown in Table 2.

4.1.2 Results Analysis

In order to study the impact of stress changes on the surrounding rock failure characteristics, different stress states are assigned by controlling the depth of the coal seam. The depths are set to 600 m, 700 m, 800 m, and 900 m respectively. The overburden rock volume is calculated at 25 kN/m^2 , the vertical stress applied to the upper part of the model is 14.5 MPa, 17 MPa, 19.5 MPa, and 22 MPa, and the horizontal stress is set to 1.2 times the vertical stress.

1. Stress analysis

Figure 8 shows the distribution of vertical stress field under different burial depths (600 m, 700 m, 800 m, 900 m).

After the roadway is excavated, there is a stress reduction area in the roof and floor of the roadway, and the stress concentration is formed in the depth of the side. The stress state of the surrounding rock is mainly compressive stress. Only in a certain depth range of the roadway floor, there is tensile stress, and the existence of tensile stress is the direct factor leading to floor heave. It can be seen from Fig. 6 that the stress is mainly concentrated in the range of 1.5–3 m from the roadway side, and the maximum stress concentration

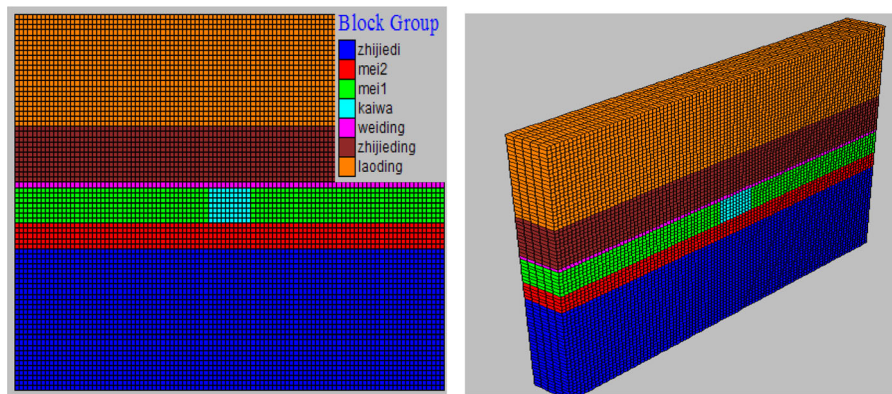


Fig. 7 Three-dimensional model

Table 2 Mechanical parameters of coal and rock mass

Rock formation	Density (kg/m ³)	Elastic modulus/GPa	Poisson's ratio	Tensile strength/MPa	Internal friction angle/°	Cohesion/MPa
Sandy mudstone	2510	3	0.147	0.75	36	2.16
Mudstone	2420	6	0.23	1.29	35	3.2
No. 21 coal seam	1500	3.5	0.38	1.25	30	1.25
Sandy	2580	9	0.123	1.84	38	2.75

coefficient is 1.26 when the depth is 600 m, the maximum stress concentration factor is 1.43 at 700 m depth, the maximum stress concentration factor is 1.56 at 800 m depth, the maximum stress concentration factor is 1.71 at 900 m depth. It can be seen that with the increase of the buried depth, the stress concentration in the roadway side increases. With the increase of the buried depth, the stress of the surrounding rock of the two sides and the roof and floor increases in varying degrees, and the peak value of the stress gradually transfers to the depth, and the bearing capacity of the surrounding rock transfers to the deep surrounding rock, thus causing a large range of damage areas.

2. Displacement analysis

The distribution law of vertical displacement field under different burial depth is shown in Fig. 9.

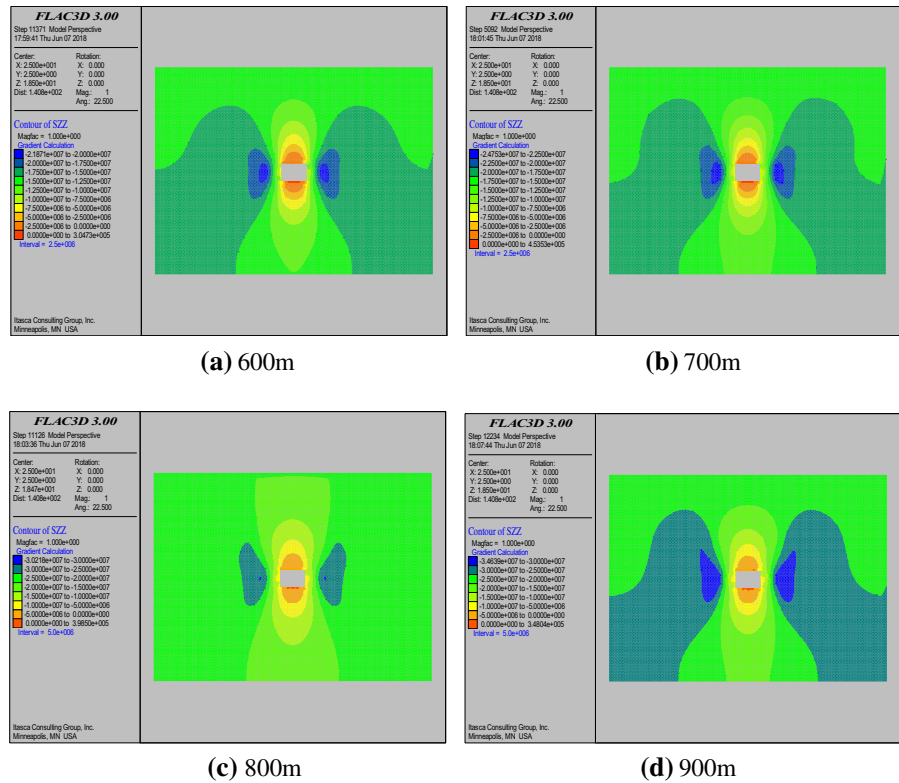
As can be seen from Fig. 9, after the roadway is excavated, the roof moves downward and the floor bulges upward. Under the condition of no support, the

maximum roof subsidence is 130 mm when the buried depth is 600 m, and the maximum floor heave is 86 mm. The maximum roof subsidence is 140 mm when the buried depth is 700 m, and the maximum floor heave is 112 mm. The maximum roof subsidence is 215 mm when the buried depth is 800 m, and the maximum floor heave is 133 mm. The maximum roof subsidence is 258 mm when the buried depth is 900 m, and the maximum floor heave is 160 mm. It shows that with the increase of buried depth, the displacement range of surrounding rock increases and the maximum displacement increases nonlinearly.

3. Plastic zone analysis

Figure 10 shows the range of plastic zone after tunnel excavation under four kinds of buried depth conditions. In the figure, none indicates that there is no tension shear failure of the unit, shear-p indicates that the unit has shear failure, shear-p indicates that the unit is shear failure, tension-p indicates that the unit has

Fig. 8 Cloud chart of vertical stress distribution under different burial depth



tensile failure, and tension-n indicates that the unit is tensile failure.

It can be seen from Fig. 10 that with the increase of burial depth, the plastic failure of the surrounding rock of the roadway gradually expands, and the failure mode is mainly shear failure. Due to the shear expansion effect of the coal and rock mass, there is a little tensile failure on the roadway surface. When the buried depth is 600 m, the plastic damage range of the two sides of the roadway and the floor is about 2 m, and the roof is about 1.5 m; when the buried depth is 700 m, the plastic damage range of the two sides of the roadway is about 2.5 m, the roof is about 2 m, and the floor is about 3 m; when the buried depth is 800 m, the plastic damage range of the two sides of the roadway is about 4 m, the roof and the floor are about 3.5 m, and the plastic area at the top and bottom corner increases obviously; when the buried depth is 900 m, the plastic damage range of the two sides of the roadway is about 2 m, and the floor is about 3 m. The damage range is about 5 m, and the top and bottom plates are about 4.5 m. Therefore, with the increase of in situ stress, the plastic range of the surrounding rock of the tunnel increases nonlinearly.

4.2 Numerical Simulation Analysis of Different Reinforcement Methods

4.2.1 Model Establishment

In order to study the effect of the original support, the anchor grouting support of the bottom plate and the cooperative reinforcement support of the side and the bottom in the bottom drum treatment, the FLAC^{3D} numerical simulation software is used to establish the three-dimensional model as shown in Fig. 7. The displacement constraints are imposed on the left, right, front, back and bottom boundaries of the model, the uniformly distributed load is applied on the top of the model, and the buried depth of the No. 11021 working face is about 700 m, then the load of 17.5 MPa is applied on the top of the model, the side pressure coefficient is taken as 1.2, the mechanical performance parameters of the coal and rock mass are shown in Table 2, and the parameters of the support components are shown in Table 3. The three-dimensional model of different reinforcement methods is shown in Fig. 11.

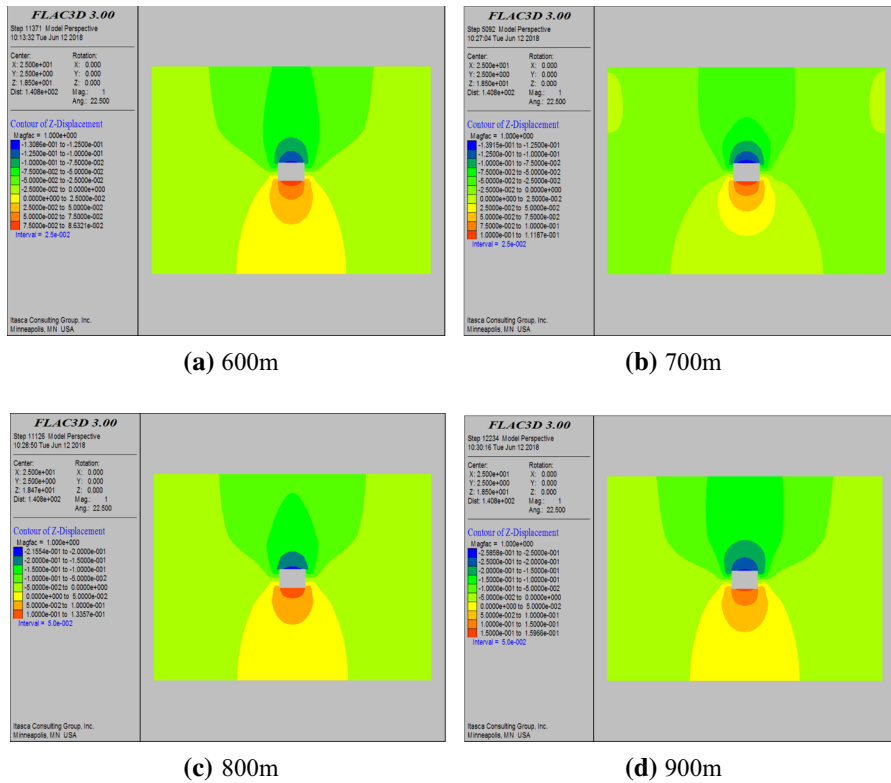


Fig. 9 Distribution law of vertical displacement field under different burial depth

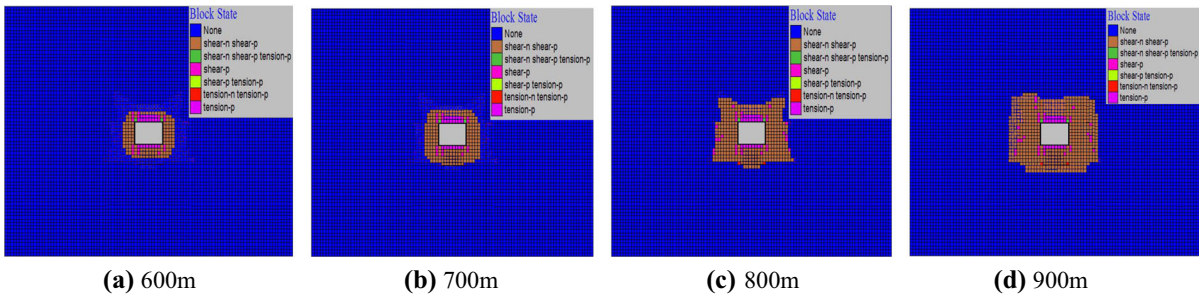
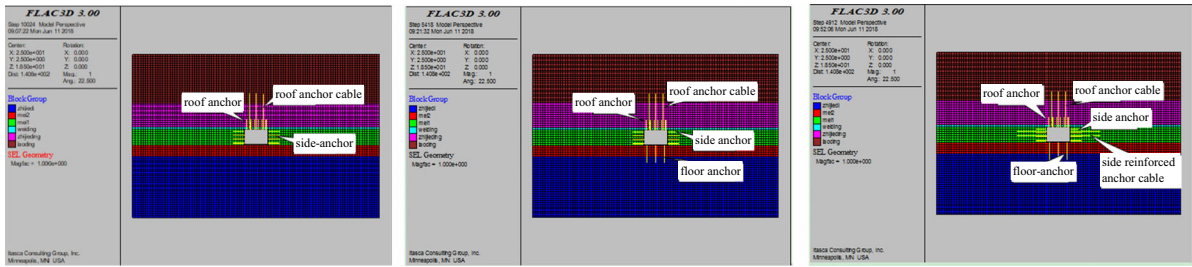


Fig. 10 Cloud diagram of plastic distribution of surrounding rock of roadway with different buried depth

Table 3 Parameters of cable structural unit

Member	Elastic modulus/ GPa	Cross section/ 10^{-4} m^2	Perimeter/ m	Cohesion/ (105 N m^{-1})	Bonding stiffness/ (107 N m^{-2})	Tensile load/ kN
Bolt	200	3.1	0.0628	4.3	2.40	228
Anchor cable	195	3.6	0.0678	1.7	1.12	607



(a) original support (b) anchor grouting support of the bottom plate (c) side-bottom cooperate to strengthen support

Fig. 11 Three dimensional model under different reinforcement methods

4.2.2 Result Analysis

1. Stress analysis

The distribution law of vertical stress field in unreinforced mode is shown in Fig. 12.

It can be seen from Fig. 12 that under the original support state, the concentrated stress distribution in the two sides of the roadway is obvious, and the maximum stress concentration coefficient is 1.48. Under the condition of reinforcement of the side and bottom, the stress concentration area of the side disappears basically, and the influence of mining activities on the original rock stress is concentrated in a small area. Without the effect of the concentration stress, the coal and rock mass in the depth of the surrounding rock remains intact, which proves that the reinforcement of the side and bottom enhances the bearing capacity of the surrounding rock of the roadway.

2. Displacement analysis

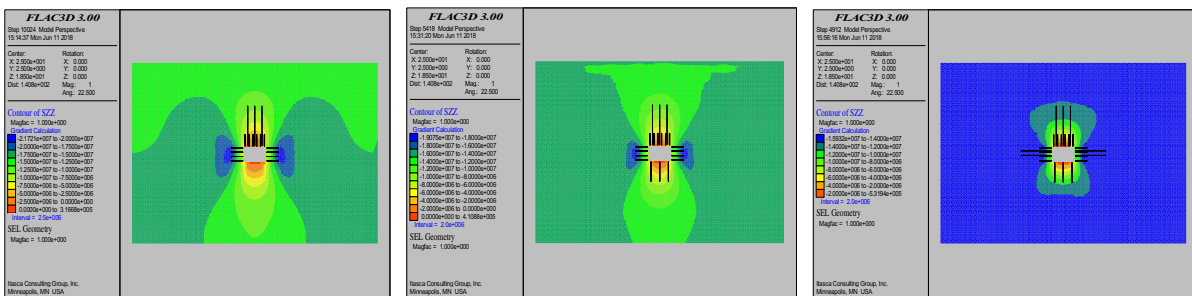
The distribution of vertical displacement field under different reinforcement methods is shown in Fig. 13.

It can be seen from Fig. 13 that under the original support state, the maximum roof subsidence is 120 mm, and the floor heave is 86 mm; under the anchor injection support state, the maximum roof subsidence is 83 mm, and the floor heave is 8 mm, and the area where the floor heave occurs is greatly reduced; under the condition of the synergetic reinforcement support of the top and bottom, the maximum roof subsidence is 65 mm, and the floor heave is only 4 mm, and the deep surrounding rock is basically in a stable state without displacement change.

3. Plastic zone analysis

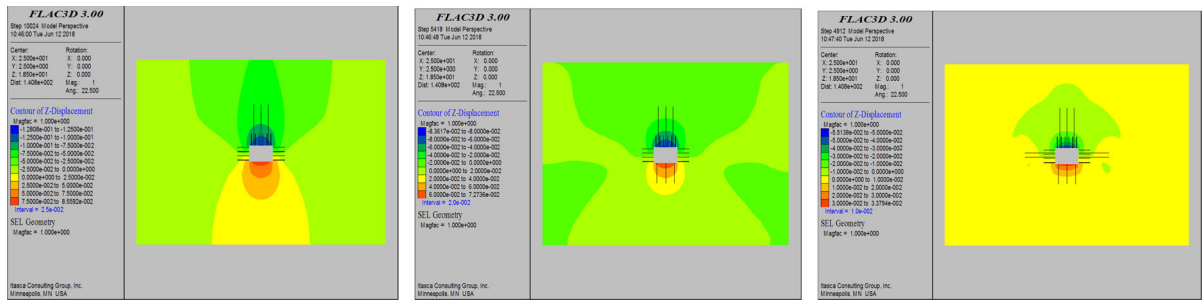
The distribution law of plastic zone in surrounding rock of roadway under different reinforcement methods is shown in Fig. 14.

It can be seen from the analysis in Fig. 14 that under the original support state, the floor without support is in the state of free surface, and the plastic failure depth of the floor under the action of in situ stress is about



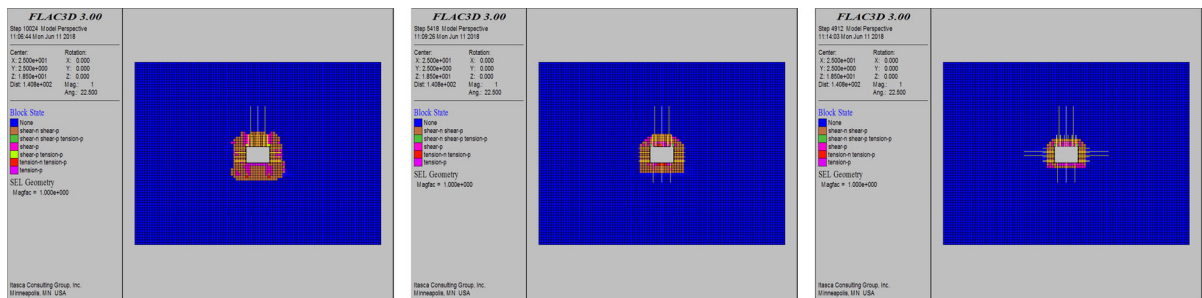
(a) original support (b) anchor grouting support of the bottom plate (c) side-bottom cooperate to strengthen support

Fig. 12 Stress field distribution under different support conditions



(a) original support (b) anchor grouting support of the bottom plate (c) side-bottom cooperate to strengthen support

Fig. 13 Vertical displacement distribution under different support conditions



(a) original support (b) anchor grouting support of the bottom plate (c) side-bottom cooperate to strengthen support

Fig. 14 Plastic zone distribution law under different support conditions

4 m, which is obviously larger than that of the roof and the side under the support state. Compared with the support without support, the plastic failure depth of the base plate is obviously reduced, which is mainly the failure of the coal body of the base plate within 2 m. In this case, the surrounding rock of the roadway forms a unified bearing body, the plastic failure area becomes smaller, and the surrounding rock of the roadway is more stable.

5 On-Site Monitoring

In the tail entry of inner section of No. 11021 working face, the displacement observation station is arranged by cross point arrangement method, as shown in Fig. 15.

In this figure, AB represents the horizontal displacement, and CD represents the roof to floor convergence. Four groups of stations are arranged every 10 m, among which 1# and 4# stations are non-bottom grouting anchor control areas, 2# and 3# stations are bottom grouting anchor control areas. And

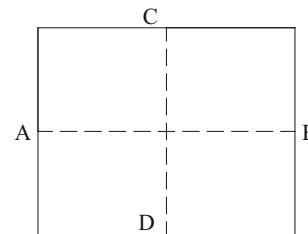


Fig. 15 Displacement observation station

draw the curve of roadway deformation with time as shown in Fig. 16.

It can be seen from Fig. 16a that the two side displacement approaches of tunnel 1#–4# measuring station in about 50 days are 318 mm, 269 mm, 231 mm and 345 mm respectively. It can be seen from Fig. 16b that the bottom heave of tunnel 1#–4# measuring station in about 50 days are 338 mm, 142 mm, 224 mm and 361 mm respectively.

It can be seen that the displacement and bottom heave of two sides in the control area (2# and 3# stations) of the bottom grouting anchor are significantly smaller than those in the non-control area (1#

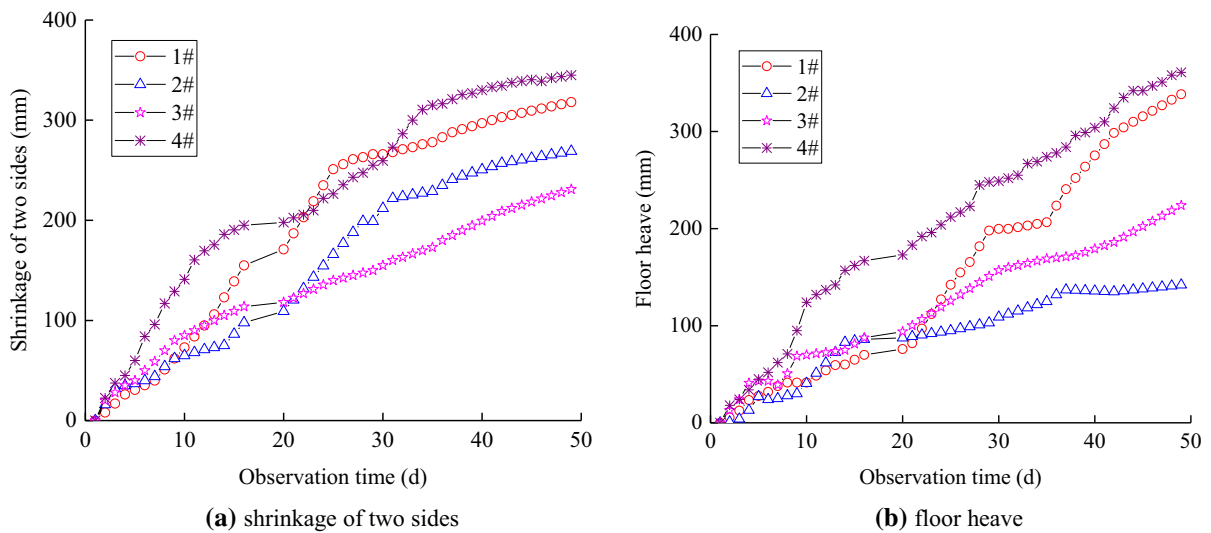


Fig. 16 Relationship curve of roadway deformation with time

and 4# stations), the displacement of two sides in three stations is about 67% of that in four stations, and the bottom heave of two stations is about 39% of that in four stations. The overall reinforcement effect of the roadway is good, the surface of the roadway is smooth, and there is no crack of concrete and bolt.

6 Conclusion

1. It is considered that the floor heave of the soft rock roadway is the result of the joint action of the surrounding rock fracture development, poor lithology, cementation, low strength of the original support and high ground stress.
2. The distribution characteristics of stress, displacement and plastic zone of surrounding rock in soft rock roadway under different stress and support mode are analyzed by numerical simulation.
3. The grouting bolt is used in the treatment of roadway floor, and a new type of floor drilling equipment is developed.
4. The combined control technology of “prestressed grouting anchor cable + grouting anchor bolt + grouting behind the wall + floor reconstruction” is proposed to effectively control the occurrence of roadway floor.

Author’s Contribution LX and SW conceived and designed the experiments; LX performed the experiments; LX and SW analyzed the data; and LX wrote the paper.

Funding This work was supported by National Natural Science Foundation of China (No. 51974104).

Compliance with Ethical Standards

Conflict of interest The authors declare no conflict of interest.

References

- Guo ZP, Du ZW, Hu SC et al (2017) Comprehensive treatment methods of floor heave disasters in mining areas of China. *Geotech Geol Eng* 5(35):2485–2495
- Hao YX, Wang J, Yuan Y et al (2016) Large deformation control technology for expansive and weak-cemented soft rock roadways in Shajihai coal mine. *J Min Saf Eng* 33(4):684–691
- He MC, Sun XM (2004) Guidelines for support design and construction of China Coal Mine Soft Rock Roadway Engineering. Science Press, Beijing
- He MC, Yuan Y, Wang XL et al (2013) Control technology for large deformation of mesozoic compound soft rock in Xinjiang and its application. *Chin J Rock Mech Eng* 32(3):433–441
- He MC, Wang J, Sun XM et al (2014) Mechanics characteristics and applications of prevention and control rock bursts of the negative Poisson’s ratio effect anchor. *J China Coal Soc* 39(2):214–221
- Kang HP, Lin J, Yang JH et al (2011) Stress distribution and synthetic reinforcing technology for chamber group with soft and fractured surrounding rock. *Chin J Geotech Eng* 33(5):808–814

- Liu KM, Gao YF, Zhang FY (2017a) Composite supporting technology of concrete filled steel tubular support in extremely soft rock roadway with large section. *J Min Saf Eng* 34(2):243–250
- Liu XN, Peng YH, Zhou T (2017b) Study on support technology of deep high stress mining tunnel. *J Henan Polytech Univ Nat Sci* 36(3):18
- Long JK, Jiang BS, Liu G et al (2012) Study on the mechanism and application of synergistic anchoring systems in roadway surrounding rocks. *J China Coal Soc* 37(3):372–378
- Ma NJ, Hou CJ (1995) Theory and application of mine pressure in mining roadway. Coal Industry Press, Beijing, p 144
- Meng QB, Han LJ, Qi B et al (2017) Study and application of key technology for roadway crossing faults under complex geological conditions. *J Min Saf Eng* 34(2):199–207
- Song WH, Shi MZ, Zhao CY et al (2018) Study on fracture zone of cross fault group in large section rectangular roadway under mining conditions. *Coal Sci Technol* 46(10):122–129
- Sun XM, He MC (2005) Numerical simulation research on coupling support theory of roadway within soft rock at depth. *J China Univ Min Technol* 34(2):37–40
- Wang WJ, Yuan C, Yu WJ et al (2016) Stability control method of surrounding rock in deep roadway with large deformation. *J China Coal Soc* 41(12):2921–2931
- Wang J, Hu CC, Zuo JP et al (2019) Mechanism of roadway floor heave and control technology in fault fracture zone. *J China Coal Soc* 44(02):53–64
- Wei SJ, Gou PF, Yu CS (2013) Creep simulation on fractured surrounding rock of large section chamber and its control technology. *J Min Saf Eng* 30(4):489–494
- Wu YZ, Chu XW, Wu JX et al (2017) Micro-mesoscopic test on fracture failure of intensive rock bolts. *J China Coal Soc* 42(3):574–581
- Yan S, Bai JB, Zhang ZZ et al (2016) Failure mechanism and ground control of a main entry above aquifers crossing fault zone. *J Min Saf Eng* 33(6):979–984
- Zhang JJ (2005) Discussion on optimization of deep mining technology. *Ground Press Strata Control* 3:74–75
- Zhang YW (2016) Study on support system optimization of broken seam and rock gateway along fault. *Coal Sci Technol* 44(09):72–76
- Zhang GF, Xie Y, Xu LY (2016a) Mechanics performance testing and research of truss support in the soft rock roadway. *J Min Saf Eng* 33(4):649–654
- Zhang GF, Wang E, Xu LY (2016b) Mechanical characteristics of high constant resistance and large deformation. *Chin J Rock Mech Eng* 35(10):2033–2043
- Zheng WX, Zhao YL, Bu QW (2018) The coupled control of floor heave based on a composite structure consisting of bolts and concrete antiarches. *Math Probl Eng* 2018:1–14

Publisher's Note Springer Nature remains neutral with regard to jurisdictional claims in published maps and institutional affiliations.